Subradiant Split Cooper Pairs

Audrey Cottet,[1] Takis Kontos,[1] and Alfredo Levy Yeyati[2]

[1]*Laboratoire Pierre Aigrain, Ecole Normale Supérieure, CNRS UMR 8551, Laboratoire associé aux universités Pierre et Marie Curie et Denis Diderot, 24, rue Lhomond, 75231 Paris Cedex 05, France*

[2]*Departamento de Física Teórica de la Materia Condensada C-V and Instituto Nicolás Cabrera, Universidad Autónoma de Madrid, E-28049 Madrid, Spain*

(Received 29 November 2011; published 20 April 2012)

We suggest a way to characterize the coherence of the split Cooper pairs emitted by a double-quantum-dot based Cooper pair splitter (CPS), by studying the radiative response of such a CPS inside a microwave cavity. The coherence of the split pairs manifests in a strongly nonmonotonic variation of the emitted radiation as a function of the parameters controlling the coupling of the CPS to the cavity. The idea to probe the coherence of the electronic states using the tools of cavity quantum electrodynamics could be generalized to many other nanoscale circuits.

DOI: 10.1103/PhysRevLett.108.166803 PACS numbers: 73.23.−b, 73.63.Fg

Entanglement is now accepted as an intriguing but available resource of the quantum world. However, it is still unclear whether this phenomenon can survive in nanoscale electronic circuits, because an electronic fluid is characterized by a complex many-body state in general. Producing and detecting entangled electronic states are therefore important goals of quantum electronics. The spin-singlet (Cooper) pairing of electrons, naturally present in conventional superconductors, appears as a very attractive source of electronic entangled states. Recently, the splitting of Cooper pairs could be demonstrated in Y junctions made out of nanowires [1–3]. But how to distinguish between a singlet state broken into a product state due to decoherence and the desired coherent singlet state is not addressed in these experiments. Here, we show that the radiative response of such devices can reveal the presence or absence of entangled states. The split Cooper pairs are shown to decouple from the electromagnetic field conveyed by a photonic cavity (subradiance) if coherent. These findings add a new twist to quantum optoelectronics, and could be applied to any source of on-demand entangled electronic states.

The analogy between a beam splitter for electronic states and a beam splitter for photons calls for the use of correlation measurements to characterize the degree of entanglement of pairs of electrons, via the noise cross correlations of the electrical current [4–10]. The use of a double-quantum-dot circuit connected to two normal electrodes and one superconducting electrode gives a practical realization of an electronic entangler and simplifies the diagnosis of entanglement from transport, as originally suggested by Recher *et al.* [7]. Nevertheless, measuring cross correlations in such a setup is a formidable task because the conditions for useful entanglement correspond to a regime where the system is almost isolated from the leads. In this case, the Cooper pair current is too small to yield measurable current fluctuations with present amplification techniques [11]. These difficulties stem from the fact that probing directly a quantum system with transport measurements is not natural since one needs the system to be open and closed at the same time. On the contrary, as known in atomic physics [12], the use of light-matter interaction is very well adapted to probe closed quantum systems. Here, we show how to use the coupling between electrons and photons from a microwave cavity, to assess the coherence of Cooper pairs emitted by a Cooper pair splitter (CPS) implemented with a double-quantum-dot circuit.

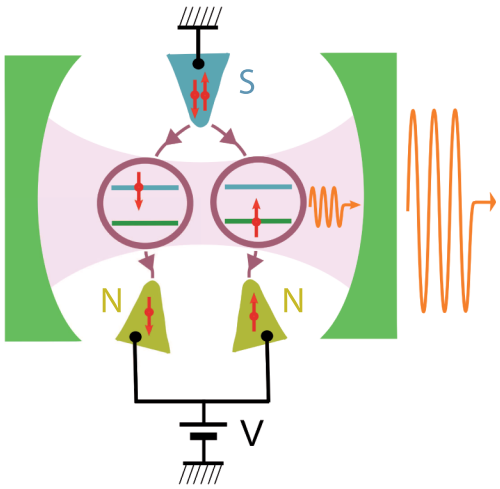

FIG. 1 (color online). Scheme of the CPS embedded in a photonic cavity. The CPS is made out of a double-quantum dot coupled to a central superconducting contact (S) connected to ground, and two outer normal metal contacts (N) biased with a voltage V. This circuit is placed inside a photonic cavity (represented schematically by mirrors). The Cooper pairs spread over the K and K' orbitals of the dots, represented by the horizontal lines in the circles. The low energy level structure of the system allows photon emission which can be amplified through a lasing effect.

We consider a CPS made out of a single wall carbon nanotube in which a double dot is defined by a central superconducting contact connected to ground and two outer normal metal contacts biased with a voltage V. This CPS is inserted inside a photonic cavity (see Fig. 1) which is assumed to be implemented in a coplanar waveguide geometry using a superconducting metal, as in the circuit quantum electrodynamics architecture [13]. Very recently, it has been demonstrated experimentally [14,15] that one can extend this architecture to quantum dot circuits [16–19], bringing our proposed setup within experimental reach.

Our aim is to find an effect which reveals qualitatively the coherent injection of Cooper pairs. Thanks to Coulomb blockade, the states participating to electronic transport can be reduced to the double-dot empty state $|0,0\rangle$, the singly occupied states $|\tau\sigma,0\rangle = d^\dagger_{L\tau\sigma}|0,0\rangle$ and $|0,\tau\sigma\rangle = d^\dagger_{R\tau\sigma}|0,0\rangle$ of the left (L) and right (R) dot, and the nonlocal doubly occupied states $|\tau\sigma,\tau'\sigma'\rangle = d^\dagger_{L\tau\sigma}d^\dagger_{R\tau'\sigma'}|0,0\rangle$, with $\tau \in \{K, K'\}$ and $\sigma \in \{\uparrow,\downarrow\}$ being orbital and spin indices, respectively (see Supplemental Material [20], part A for details). For biasing conditions like the one depicted in Fig. 1 with $eV < \Delta$ (Δ being the gap of the superconducting contact) Cooper pairs are injected from the superconductor into a singlet state $|\mathcal{S}\rangle$. The coupling to the superconductor hybridizes the $|\mathcal{S}\rangle$ state with the empty state $|0,0\rangle$ forming two states which we call $|V_1\rangle$ and $|V_2\rangle$. These states can relax to a single particle state via electron tunneling into the normal leads, and then via a second tunneling process into the state $|V_1\rangle$ or $|V_2\rangle$, which closes the usual operation loop of the CPS, as depicted in Fig. 2(b). However, when the CPS is placed in the resonant cavity there is an additional transition to a triplet state (two electronic states with equal spin) through the emission of a cavity photon. It is the aim of this work to study these photon emission processes and show that they can be used to characterize the coherence of the split pairs injected into the CPS.

The relevant energy scales of the CPS are the position ε of the energy levels on each dot, which we assume symmetric for the sake of simplicity, the Cooper pair coherent splitting rate $t_{\rm eh}$ [21,22], the effective spin-orbit coupling constant $\Delta_{\rm so}$, and the coupling between the K and K' orbitals, $\Delta_{K\leftrightarrow K'}$, which arise from weak disorder in the nanotube [23–26]. For $t_{\rm eh} = 0$, $\Delta_{\rm so} = 0$, and $\Delta_{K\leftrightarrow K'} = 0$, the doubly occupied states cost an energy $2\varepsilon = \delta$. For $t_{\rm eh} \ll \Delta_{K\leftrightarrow K'}, \Delta_{\rm so}$ [1], the regime $\delta \sim 2\Delta_r$, with $\Delta_r = \sqrt{\Delta^2_{\rm so} + \Delta^2_{K\leftrightarrow K'}}$, is the most adequate for producing entangled states. It allows one to isolate, in the double-dot even charge sector, a subset $\mathcal{E}$ of five lowest energy eigenstates which are at a distance $\sim 2\Delta_r$ from the other even charge states, at least. These five states include three spin-triplet states $|T_0\rangle$, $|T_+\rangle$, and $|T_-\rangle$ with energy $E_{\rm triplet} = \delta - 2\Delta_r$ and the two hybridized even states [27,28] $|V_n\rangle = \sqrt{1-v_n^2}|0,0\rangle + v_n|\mathcal{S}\rangle$ with energy $E_i = \frac{1}{2}(\delta - 2\Delta_r - (-1)^n\sqrt{8t^2_{\rm eh} + (\delta - 2\Delta_r)^2})$ for $n \in \{1,2\}$ (see [20], part B.4, for the expression of the $v_n's$). Here, the definition of the spin-singlet state $|\mathcal{S}\rangle$ and the spin triplets takes into account the twofold orbital degeneracy of each dot (see [20], part B.4). The energies of $|V_1\rangle$ and $|V_2\rangle$ show an anticrossing with a width $E_p = 2\sqrt{2}t_{\rm eh}$ at $\delta = 2\Delta_r$, while the energy of the triplets lies in the middle [see Fig. 2(a)].

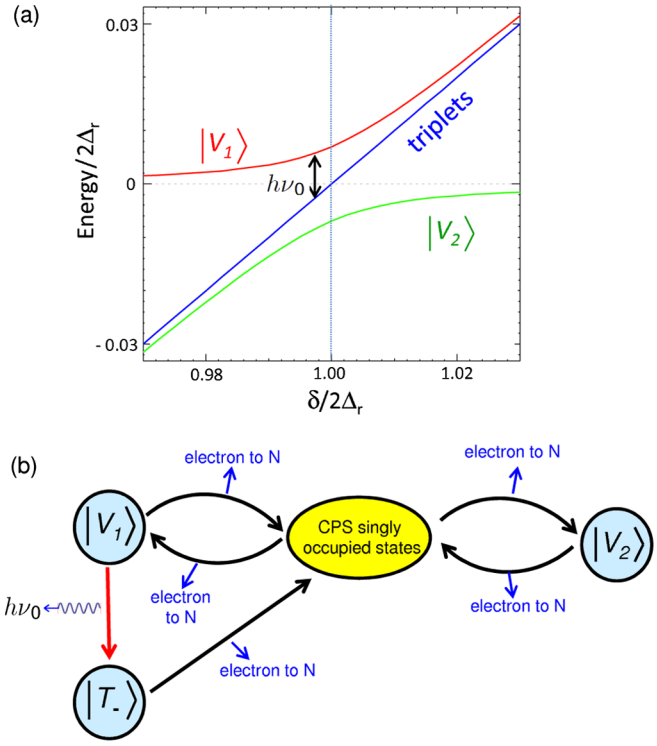

FIG. 2 (color online). (a) Spectrum of the subset $\mathcal{E}$ of even charge states of the CPS near $\delta = 2\Delta_r$. It comprises three spin-triplet states, and two states $|V_1\rangle$ and $|V_2\rangle$ which are a coherent mixture of the empty state and a spin-singlet state $|\mathcal{S}\rangle$. (b) Dynamics of the CPS near the working point $\delta = 2\Delta_r$. We consider a bias voltage regime such that the various transitions between the CPS states occur together with the transfer of one electron towards the normal contacts, apart from the transition from $|V_1\rangle$ to the triplet state $|T_-\rangle$, which occurs due to the emission of a photon towards the cavity. We have checked that the radiative transition from $|T_-\rangle$ to $|V_2\rangle$ is not active in the regime of parameters we consider.

Let us first discuss the current $I_{\rm CPS}$ through the superconducting lead, without considering the effect of the photonic cavity. We call Γ_N the bare tunnel rate of an electron between one dot and the corresponding normal metal contact, while P_A denotes the probability of a state $|A\rangle$ of the double-dot even charge sector and $P_{\rm single}$ the global probability of having a double-dot singly occupied state. In the sequential tunneling limit $\Gamma_N \ll k_BT$, these probabilities follow a master equation $\frac{d}{dt}P = MP$ with

$$P = \begin{bmatrix} P_{V_1} \\ P_{V_2} \\ P_{T_-} \\ P_{\text{single}} \end{bmatrix}, \quad \frac{M}{\Gamma_N} = \begin{bmatrix} -2v_1^2 & 0 & 0 & 1-v_1^2 \\ 0 & -2v_2^2 & 0 & 1-v_2^2 \\ 0 & 0 & -2 & 0 \\ 2v_1^2 & 2v_2^2 & 2 & -1 \end{bmatrix}. \tag{1}$$

Equation (1) corresponds to a bias voltage regime such that single electrons can go from the double dot to the normal leads but not the reverse (see [20], part C). We disregard the states $|T_0\rangle$ and $|T_+\rangle$, which are not populated in the simple limit we consider. The states $|V_i\rangle$ and $|T_-\rangle$ can decay towards several different singly occupied states. The sum of the corresponding transition rates equals $2\Gamma_N v_i^2$ and $2\Gamma_N$, respectively, which explains the presence of the factors 2 in the three first columns of M. To calculate I_{CPS}, one first has to determine the stationary value P_{stat} of P from $MP_{\text{stat}} = 0$. Then, one can use $I_{\text{CPS}} = R.P_{\text{stat}}$ with $R = e\Gamma_N[2v_1^2, 2v_2^2, 2, 1]$. If the double dot is initially in the state $|V_n\rangle$, with $n \in \{1, 2\}$, there can be a transition to a singly occupied state while an electron is transferred to the normal leads, because $|V_n\rangle$ has a $|\mathcal{S}\rangle$ component. Then, there can be a transition from this singly occupied state to $|V_m\rangle$, with $m \in \{1, 2\}$, because $|V_m\rangle$ has a $|0, 0\rangle$ component. This leads to the existence of state cycles which produce a flow of electrons towards the normal leads [see Fig. 2(b)]. On the left (right) of the anticrossing point $\delta = 2\Delta_r$, the state $|V_{1(2)}\rangle$ is the most probable. Exactly at the anticrossing point, the states $|V_1\rangle$ and $|V_2\rangle$ contribute equally to current transport and I_{CPS} is maximum (see Fig. 3, main frame).

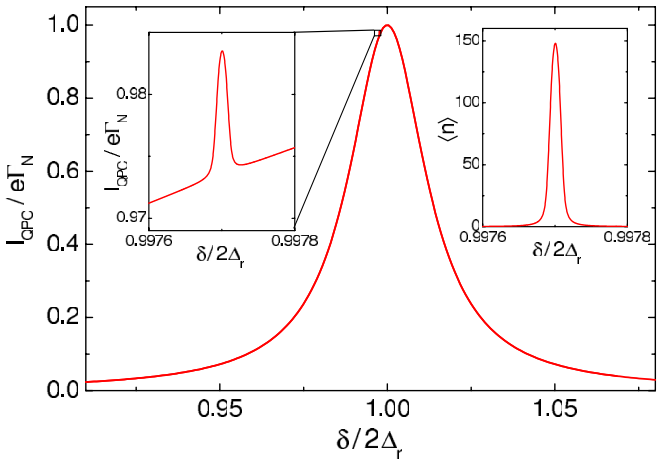

FIG. 3 (color online). Main frame: current I_{QPC} at the input of the Cooper pair splitter. The peak at $\delta = 2\Delta_r$ is due to the anticrossing between $|V_1\rangle$ and $|V_2\rangle$. Left inset: zoom on the current peak due to lasing transitions between the $|V_1\rangle$ and $|T_-\rangle$ states. Right inset: number of photons versus δ. We have used realistic parameters $t_{\text{eh}} = 9\ \mu\text{eV}$, $\Delta_{\text{so}} = 0.15$ meV, $\Delta_{K/K'} = 0.9$ meV, $\nu_0 = 3.64$ GHz, $Q = 2\pi\hbar\nu_0/\kappa = 500\,000$, $D_{pq}^{-1} = 92$ ns, $\Gamma_N = 72$ MHz, $T = 35$ mK, and $|\lambda_L - \lambda_R| = 2.5 \times 10^{-6}\Delta_r \simeq 0.55$ MHz.

Electronic spins are naturally coupled to photons thanks to the spin-orbit interaction, which exists in many types of conductors, including those used to demonstrate Cooper pair splitting. In our case, we will take into account a spin-photon coupling with the form (see [20], part F)

$$H_{\text{so}} = (a + a^\dagger) \sum_{i,\tau,\sigma} \lambda_{i\sigma} d_{i\tau\sigma}^\dagger d_{i\tau\bar{\sigma}} = (a + a^\dagger) h_{\text{so}} \tag{2}$$

with $d_{i\tau\sigma}^\dagger$ the creation operator for an electron with spin σ in orbital τ of dot $i \in \{L, R\}$ and $a^\dagger$ the creation operator for cavity photons. We use $\lambda_{i\sigma} = \mathbf{i}\sigma\lambda_i$. Inside the $\mathcal{E}$ subspace, the term H_{so} couples $|V_n\rangle$ to $|T_-\rangle$ only, i.e., for $n \in \{1, 2\}$,

$$\langle T_-|h_{\text{so}}|V_n\rangle = v_n \frac{\Delta_{K\leftrightarrow K'}}{\Delta_r} \mathbf{i}(\lambda_L - \lambda_R), \tag{3}$$

whereas $\langle T_{+[0]}|h_{\text{so}}|V_{1(2)}\rangle = 0$. The presence of the minus sign in Eq. (3) is crucial. It reveals the *coherent* injection of singlet pairs inside the CPS. If $|V_n\rangle$ was resulting from the hybridization of a product spin state with the $|0, 0\rangle$ state, the matrix element (3) would depend only on λ_L or λ_R. We will show below that the peculiar structure of the element (3) can be revealed by measuring the lasing effect associated to the transition $|V_1\rangle \rightarrow |T_-\rangle$.

In order to study current transport and the photonic dynamics simultaneously, one can generalize the above master equation description by using a semiquantum description of lasing [29]. This consists in adding inside the matrix M rates accounting for photonic emission and absorption processes, i.e., $M \rightarrow M + M_{\text{ph}}$ with

$$M_{\text{ph}} = \begin{bmatrix} 0 & 0 & W_{V_1T_-} & 0 \\ 0 & -W_{T_-V_2} & 0 & 0 \\ 0 & W_{T_-V_2} & -W_{V_1T_-} & 0 \\ 0 & 0 & 0 & 0 \end{bmatrix} \langle n \rangle + \begin{bmatrix} -W_{V_1T_-} & 0 & 0 & 0 \\ 0 & 0 & W_{T_-V_2} & 0 \\ W_{V_1T_-} & 0 & -W_{T_-V_2} & 0 \\ 0 & 0 & 0 & 0 \end{bmatrix} (\langle n \rangle + 1) \tag{4}$$

and $\langle n \rangle$ the average number of photons in the cavity. The master equation must be solved self-consistently with a photonic balance equation

$$0 = P_{V_1} W_{V_1T_-}(\langle n \rangle + 1) - P_{V_2} W_{T_-V_2} \langle n \rangle + P_{T_-}[W_{T_-V_2}(\langle n \rangle + 1) - W_{V_1T_-}\langle n \rangle] - \kappa(\langle n \rangle - \langle n \rangle_{\text{th}}), \tag{5}$$

with $\langle n \rangle_{\text{th}} = (\exp(\hbar\omega_0/k_BT) - 1)^{-1}$. The photonic transition rates $W_{V_1T_-}$ and $W_{T_-V_2}$ appearing in the above equations can be expressed as

$$W_{pq} = \frac{2|\langle p|h_{\text{so}}|q\rangle|^2(\frac{\kappa}{2} + D_{qp})}{(E_p - E_q - 2\pi\hbar\nu_0)^2 + (\frac{\kappa}{2} + D_{qp})^2} \tag{6}$$

where κ is the damping rate of the resonator and D_{qp} the decoherence rate associated to the $p \leftrightarrow q$ resonance. The above description is valid provided the transitions $|V_1\rangle \rightarrow |T_-\rangle$ and $|T_-\rangle \rightarrow |V_2\rangle$ are not both resonant with the cavity; i.e., one does not have simultaneously $\delta = 2\Delta_r$ and $2\pi\hbar\nu_0 = \sqrt{2}t_{\rm eh}$. The left inset of Fig. 3 shows a zoom on $I_{\rm CPS}$ around $\delta = \delta_l(\nu_0) = 2\Delta_r - 2\pi\hbar\nu_0 + (t_{\rm eh}^2/\pi\hbar\nu_0)$. A current peak occurs at $\delta = \delta_l(\nu_0)$, due to the lasing effect which involves the $|V_1\rangle \rightarrow |T_-\rangle$ transition. Note that the population inversion necessary for the lasing effect is achieved without any ac excitation thanks to the dc bias voltage. The tunnel transition rate from $|T_-\rangle$ to the singly occupied states is larger than the transition rate from $|V_1\rangle$ to the singly occupied states [see Eq. (1)], which explains the increase in $I_{\rm CPS}$ while the system lases. However, for typical parameters, the current peak due to lasing corresponds to $\sim$100 fA over a strong background of $\sim$10 pA. The lasing effect is more clearly visible through the average number $\langle n\rangle$ of photons in the cavity, which can be measured with microwave amplification techniques [30] (see right inset of Fig. 3).

The peculiar shape of the matrix element (3) is particularly interesting if one can tune independently the couplings $\lambda_{L(R)}$, e.g., tune λ_L while λ_R remains constant (see [20], part F.2). The main frame of Fig. 4 shows $\langle n\rangle$ versus λ_L. Strikingly, this curve is not monotonic. When λ_L is too close to λ_R, the average number of photons in the cavity collapses, because the element $\langle T_-|h_{\rm so}|V_n\rangle$ becomes too small. Two lasing thresholds appear, one for $\lambda_L < \lambda_R$ and one for $\lambda_L > \lambda_R$. This nonmonotonic behavior is directly

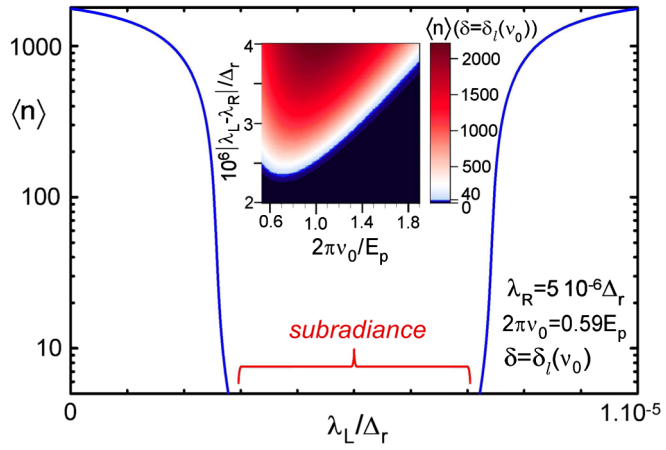

FIG. 4 (color online). Main frame: number $\langle n\rangle$ of photons in the cavity for the same parameters as in Fig. 3, as a function of the coupling λ_L, for constant values of δ and λ_R. The vanishing of $\langle n\rangle$ for small values of $|\lambda_L - \lambda_R|$ is a direct signature of coherent injection of split Cooper pairs inside the CPS. Inset: maximum number of photons which can be obtained at $\delta = \delta_l(\nu_0)$, as a function of the cavity frequency ν_0 and $|\lambda_L - \lambda_R|$. If $|\lambda_L - \lambda_R|$ is sufficiently large, the lasing effect can be obtained for a broad range of ν_0.

due to the presence of the minus signs in Eq. (3) and it therefore represents a smoking gun for coherent Cooper pair injection inside the device. Note that for a typical CPS, the range of cavity frequency ν_0 leading to the lasing effect is rather broad, because the parameter δ can be tuned to $\delta_l(\nu_0)$ with the dots' gate voltages. The inset of Fig. 4 shows the maximum number of photons in the cavity, obtained at $\delta = \delta_l(\nu_0)$, as a function of ν_0 and $|\lambda_L - \lambda_R|$. For the parameters of Fig. 3 and in particular $|\lambda_L - \lambda_R| = 2.5 \times 10^{-6}\Delta_r$, the range 3.3 GHz $< \nu_0 <$ 5.9 GHz allows one to have $\langle n\rangle \geq 40$. Interestingly, for $\delta_r > 2\Delta_r$, the state $|V_2\rangle$ is more probable than $|V_1\rangle$, but it cannot produce any lasing effect. In this case, one can imagine to test the existence of the minus sign in Eq. (3) by applying to the CPS a classical ac gate voltage with frequency $(E_{\rm triplet} - E_2)/2\pi\hbar$ instead of coupling it to the electric field of a cavity. The current through the CPS should show a nonmonotonic dependence with respect to λ_L or λ_R. However, the current variations corresponding to this effect might be very small. The lasing effect discussed in this Letter presents the advantage of providing an intrinsic and powerful amplification mechanism for the coefficient $\langle T_-|h_{\rm so}|V_1\rangle$. This contrasts with a previous proposal where a cavity was not used [31].

Before concluding, we discuss our findings on a more general level. In principle, spin-flip processes induced by the magnetic coupling $g_{L(R)}$ between the cavity photons and spins in dot $L(R)$ can also lead to the subradiance effect. Using a generic single orbital model for each dot, which leads to CPS doubly occupied states $|\sigma, \sigma'\rangle$, we find transition amplitudes between the singlet state $|\downarrow,\uparrow\rangle - |\uparrow,\downarrow\rangle$ and the triplet states $|\uparrow,\uparrow\rangle$ and $|\downarrow,\downarrow\rangle$ which are directly proportional to $g_L - g_R$. This illustrates that the subradiance phenomenon studied here is a property of the injected states rather than of the spin-photon coupling mechanism. Nevertheless, in practice, $g_{L(R)}$ is expected to be extremely small [32]. One thus has to consider a spin-photon coupling term mediated by the cavity electric field, like, e.g., the term of Eq. (2) caused by spin-orbit coupling. In principle, our findings can be generalized to other types of quantum dots with spin-orbit coupling like InAs quantum dots (see, e.g., Ref. [33]), but the detailed analysis of these cases goes beyond the scope of the present work. In our case, we have found a coupling element (3) which vanishes for $\Delta_{K\leftrightarrow K'} = 0$. However, $\Delta_{K\leftrightarrow K'} \neq 0$ is not a fundamental constraint to obtain a subradiant lasing transition. Indeed, at another working point $\delta \sim -2\Delta_r$, we find a third hybridized even state $|V_3\rangle = \sqrt{1 - v_3^2}|0, 0\rangle + v_3|\mathcal{S}\rangle$ which can decay radiatively to a triplet state $|T_a\rangle$. One can check that the coupling element $\langle T_a|h_{\rm so}|V_3\rangle$ has a subradiant form but remains finite for $\Delta_{K\leftrightarrow K'} = 0$. Here, we have chosen to discuss the lasing transition $|V_1\rangle \rightarrow |T_-\rangle$ at $\delta = \delta_l(\nu_0) \sim 2\Delta_r$ because its frequency is more likely to match with a microwave cavity resonance frequency in practice (see [20], section D for details).

In conclusion, we have shown that the coherence of entangled states produced by a Cooper pair splitter can be proven by the lasing properties of the device when coupled to a microwave cavity. The idea to probe the coherence of electronic states using the tools of cavity QED could be generalized to many other nanoscale circuits.

We acknowledge fruitful discussions with J. M. Raimond, J. Klinovaja, and B. Braunecker. This work was financed by the EU-FP7 Project No. SE2ND[271554].

[1] L. G. Herrmann, F. Portier, P. Roche, A. Levy Yeyati, T. Kontos, and C. Strunk, Phys. Rev. Lett. **104**, 026801 (2010).
[2] L. Hofstetter, S. Csonka, J. Nygard, and C. Schönenberger, Nature (London) **461**, 960 (2009).
[3] L. Hofstetter, S. Csonka, A. Baumgartner, G. Fülöp, S. d'Hollosy, J. Nygård, and C. Schönenberger, Phys. Rev. Lett. **107**, 136801 (2011).
[4] T. Martin, Phys. Lett. A **220**, 137 (1996).
[5] M. P. Anantram and S. Datta, Phys. Rev. B **53**, 16 390 (1996).
[6] G. Burkard, D. Loss, and E. V. Sukhorukov, Phys. Rev. B **61**, R16 303 (2000).
[7] P. Recher, E. V. Sukhorukov, and D. Loss, Phys. Rev. B **63**, 165314 (2001).
[8] G. B. Lesovik, T. Martin, and G. Blatter, Eur. Phys. J. B **24**, 287 (2001).
[9] J. Borlin, W. Belzig, and C. Bruder, Phys. Rev. Lett. **88**, 197001 (2002).
[10] P. Samuelsson and M. Büttiker, Phys. Rev. Lett. **89**, 046601 (2002).
[11] J. Wei and V. Chandrasekhar, Nature Phys. **6**, 494 (2010).
[12] J.-M. Raimond, M. Brune, and S. Haroche, Rev. Mod. Phys. **73**, 565 (2001).
[13] A. Wallraff, D. I. Schuster, A. Blais, L. Frunzio, R.- S. Huang, J. Majer, S. Kumar, S. M. Girvin, and R. J. Schoelkopf, Nature (London) **431**, 162 (2004).
[14] M. R. Delbecq, V. Schmitt, F. D. Parmentier, N. Roch, J. J. Viennot, G. Fève, B. Huard, C. Mora, A. Cottet, and T. Kontos, Phys. Rev. Lett. **107**, 256804 (2011).
[15] T. Frey, P. J. Leek, M. Beck, A. Blais, T. Ihn, K. Ensslin, and A. Wallraff, Phys. Rev. Lett. **108** 046807 (2012).
[16] L. Childress, A. S. Sørensen, and M. D. Lukin, Phys. Rev. A **69**, 042302 (2004).
[17] A. Cottet and T. Kontos, Phys. Rev. Lett. **105**, 160502 (2010).
[18] A. Cottet, C. Mora, and T. Kontos, Phys. Rev. B **83**, 121311(R) (2011).
[19] P.-Q. Jin, M. Marthaler, J. H. Cole, A. Shnirman, and G. Schön, Phys. Rev. B **84**, 035322 (2011).
[20] See Supplemental Material at http://link.aps.org/supplemental/10.1103/PhysRevLett.108.166803 for more details on the CPS Hamiltonian description, the coupling term of Eq. (2) and its effects, the bias voltage window to use, and other lasing transitions possible in our device.
[21] J. Eldridge, M. G. Pala, M. Governale, and J. König, Phys. Rev. B **82**, 184507 (2010).
[22] P. Burset, W. J. Herrera, A. Levy Yeyati, Phys. Rev. B **84**, 115448 (2011).
[23] T. S. Jespersen, K. Grove-Rasmussen, J. Paaske, K. Muraki, T. Fujisawa, J. Nygård, and K. Flensberg, Nature Phys. **7**, 348 (2011).
[24] W. Liang, M. Bockrath, and H. Park, Phys. Rev. Lett. **88**, 126801 (2002).
[25] F. Kuemmeth, S. Ilani, D. C. Ralph, and P. L. McEuen, Nature (London) **452**, 448 (2008).
[26] A. Pályi and G. Burkard, Phys. Rev. Lett. **106**, 086801 (2011).
[27] P. Recher, Y. V. Nazarov, and L. P. Kouwenhoven, Phys. Rev. Lett. **104**, 156802 (2010).
[28] F. Godschalk, F. Hassler, and Y. V. Nazarov, Phys. Rev. Lett. **107**, 073901 (2011).
[29] S. André, V. Brosco, M. Marthaler, A.Shnirman, and G. Schön, Phys. Scr. **T137**, 014016 (2009).
[30] O. Astafiev, K. Inomata, A. O. Niskanen, T. Yamamoto, Yu. A. Pashkin, Y. Nakamura, and J. S. Tsai, Nature (London) **449**, 588 (2007).
[31] V. Cerletti, O. Gywat, and D. Loss, Phys. Rev. B **72**, 115316 (2005).
[32] A. Imamoğlu, Phys. Rev. Lett. **102**, 083602 (2009).
[33] M. Eto and T. Yokoyama, J. Phys. Soc. Jpn. **79**, 123711 (2010).